Eur. Phys. J. D **9**, 445–450 (1999)

THE EUROPEAN PHYSICAL JOURNAL D

EDP Sciences

Surface effects in order–disorder transformations in molecular clusters

A. Proykova[1,2] and R.St. Berry[3]

[1] University of Sofia, Faculty of Physics, BG-1126 Sofia, Bulgaria
[2] Institute for Nuclear Theory, University of Washington, Box 351550, Seattle, WA 98195, USA
[3] The University of Chicago, Department of Chemistry Chicago, IL 60637, USA

Received: 2 September 1998 / Received in final form: 18 November 1998

Abstract. The effect of a surface on structural phase transitions in clusters is examined by means of velocity autocorrelation functions for TeF_6 clusters. Isothermal molecular dynamics via quaternion-based equations of motion reveals two successive phase transitions in this plastic substance. The lower-temperature transition is continuous, associated with rotational ordering. The other transition involves translation–rotation coupling in which the growth of correlations causes a crossover from a displacive to an order–disorder regime. Both the linear and angular autocorrelation functions show negative regions at low temperatures. The negative portion of the linear velocity autocorrelation function arises from the system's memory in the rebound of a molecule against its shell of neighbors. The negative part of the angular velocity autocorrelation function is ascribed to librations of the molecules in their close-packed cages. At still lower temperatures, the negative part exhibits two minima, which are best resolved when linear velocity autocorrelation functions are plotted separately for the surface and the volume molecules. This indicates different memories for surface and volume molecules.

PACS. 36.40.Ei Phase transitions in clusters – 64.70.Kb Solid-solid transitions

1 Introduction

In recent publications [1–3] we described the solid–solid transformation of plastic molecular nanoclusters to try to understand under which conditions this transformation is a finite-system precursor of a continuous, second-order transition of the limiting bulk solid. The orientationally disordered substance consists of molecules that are nearly spherical in shape [4]. The disordered phase appears at high temperatures and often has a simple structure, such as a face-centered or body-centered cubic structure. As the temperature of an orientationally disordered crystal is lowered, a phase transition to a more ordered phase takes place, and is characterized by a lower-symmetry crystal structure and the onset of long-range orientational order. The transition may be continuous or weakly discontinuous. Sometimes there are successive transitions such as we have detected in our simulations of tellurium hexafluoride clusters [1]. As the temperature decreases from the cluster's melting region, it undergoes two transformations: First, such a cluster transforms from a bcc to a monoclinic structure with partial disorder; then, at a lower temperature, it transforms to an orientationally ordered base-centered monoclinic structure. In the higher-temperature transition, rotation–translation coupling may occur in real systems, leading to a displacive component. This crossover from a disorder–order to a displacive regime is a phenomenon typical of plastic substances. All orientationally disordered crystals show some degree of translation–rotation coupling for some phonons, but the importance of the coupling varies. For bulk systems, one usually predicts which phonons are coupled to which kind of order on the basis of symmetry arguments. Unfortunately, most of the symmetries that aid analyses of bulk systems are broken in the free-surface nanoclusters. Thus, other techniques must be implemented to further the understanding of how the ordering process in a small system occurs.

Various experiments have been performed toward the understanding of the ordering processes in SF_6, SeF_6, TeF_6, and CBr_4 [5–8]. In many cases, the form observed in a supersonic jet depends upon the conditions of expansion [9]. Very small clusters are molten at much lower temperatures than the bulk melting point [12]. The fact that the crystalline structures are the only form observed of these molecular clusters indicates that they undergo a structural transformation during their growth to a final size of 10^3 to 10^4, which is typical for such experiments. At this size, the clusters of polyatomic molecules assume the crystalline structures seen in the bulk. That the bulk structure occurs for such small clusters is a consequence of the anisotropic intermolecular potential. Molecular dynamics simulations have shown that very small molecular clusters (the 19-molecule SF_6 cluster [10] and the 27-molecule TeF_6 cluster [11]) can exhibit the bulk phases. In contrast, the experiments performed in Orsay [13, 14] have shown that argon clusters exhibit an amorphous, polytetrahedral, or

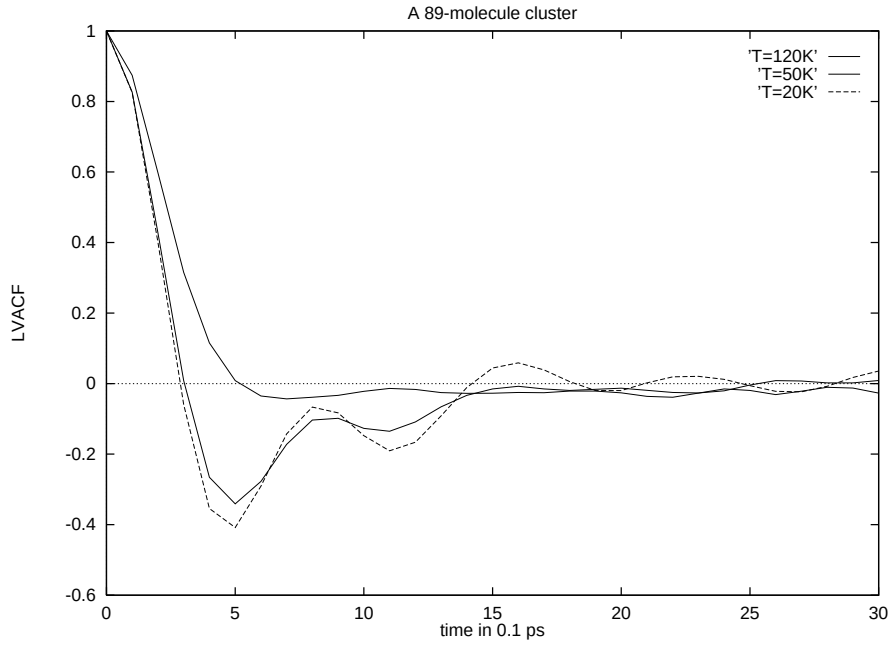

Fig. 1. The LVACF for an 89-molecule TeF_6 cluster at three selected temperatures: $T = 120\,\mathrm{K}$ (solid line); $T = 50\,\mathrm{K}$ (dashed line) below the first transition; and $T = 20\,\mathrm{K}$ (short-dashed line) below the second transition.

polyicosahedral form when they are small, and only begin to adopt their bulk structure when they reach a size of at least 1000 atoms.

The aim of this article is to show the role of the surface in the ordering process, which takes place in a disorder–order transformation of free clusters consisting of rigid octahedral TeF_6 molecules. This aim is achieved by the analysis of some dynamical properties, namely the linear and angular velocity autocorrelation functions, LVACF and AVACF, respectively.

The results obtained here might encourage a Raman investigation of finite-size molecular clusters, which will give insight of how the symmetry breaking due to the free surface contributes to appearance of rotation–translation coupling. We remind the reader that the general theory does not predict such coupling for a bulk system of octahedral molecules arranged in a body-centered cubic structure [17].

2 Computational details

The octahedral molecules of TeF_6 are considered as rigid bodies with the length of the Te−F bond 1.81 Å. The anisotropy of the intermolecular interaction is accounted for by a sum of pairwise Lennard–Jones and Coulomb atom–atom interactions:

$$U = \sum_{i<j}^{N} \sum_{\alpha,\beta}^{7} 4\varepsilon_{\alpha\beta} \left[(\sigma_{\alpha\beta}/r_{ij})^{12} - (\sigma_{\alpha\beta}/r_{ij})^{6} \right] + q_{i\alpha} q_{j\beta} / r_{ij}, \tag{1}$$

where r_{ij} is the distance between the ith and the jth atom. The indices α and β denote either a fluorine or a tellurium atom. The values for $\sigma_{\alpha\beta}$ and $\varepsilon_{\alpha\beta}$ are chosen to be [9]: $\sigma_{\mathrm{Te–Te}} = 4.29\,\text{Å}$, $\sigma_{\mathrm{Te–F}} = 3.55\,\text{Å}$, $\sigma_{\mathrm{F–F}} = 2.94\,\text{Å}$ $\varepsilon_{\mathrm{Te–Te}} = 1.376\,\mathrm{kJ/mol}$, $\varepsilon_{\mathrm{Te–F}} = 0.531\,\mathrm{kJ/mol}$, and $\varepsilon_{\mathrm{F–F}} = 0.205\,\mathrm{kJ/mol}$. The Coulomb interaction accounts for the observed electronegativity of the fluorine atoms with a partial charge of 0.1e placed at the atomic center.

The classical equations of motion for a cluster of N molecules interacting via the potential (1) are written in Hamiltonian form and integrated using the velocity Verlet algorithm with 10 fs time steps; this preserves the total energy up to 10^{-5}. The model for the potential function and the cluster has been shown to reproduce the solid–solid transformations as a function of the cluster temperature. For the cluster sizes we studied, we have found two successive transitions in our simulations [1, 3] of the TeF_6 clusters as they are cooled from their size-dependent melting point. The first transition, which is detected in the temperature interval 60–100 K, depending on the cluster size, involves translation–rotation coupling in which growth of correlations with cluster size drives a crossover from a displacive (discontinuous) to an order–disorder (continuous) regime. The other transition, at a temperature below 40 K, is continuous, associated with rotational ordering of the molecular axes of symmetry [2]. In other words, the upper transition changes with cluster size from the finite-system counterpart of first order to the counterpart of second order (continuous), while the lower transition is a counterpart of a second-order transition for small system. It is expected that in bulk, the metastable structure recognized at the higher transition in clusters does not exist.

An inherent difficulty of the molecular dynamics computations is that the shapes of the correlation functions cannot be simply adjusted when the potential parameters are changed. The ability to reproduce experimental dynamical properties is a test of a potential model fitted to equilibrium properties. A fundamental requirement for this type of study is the availability of accurate experimental data. The single-molecule reorientational time can be measured as a function of the temperature by the

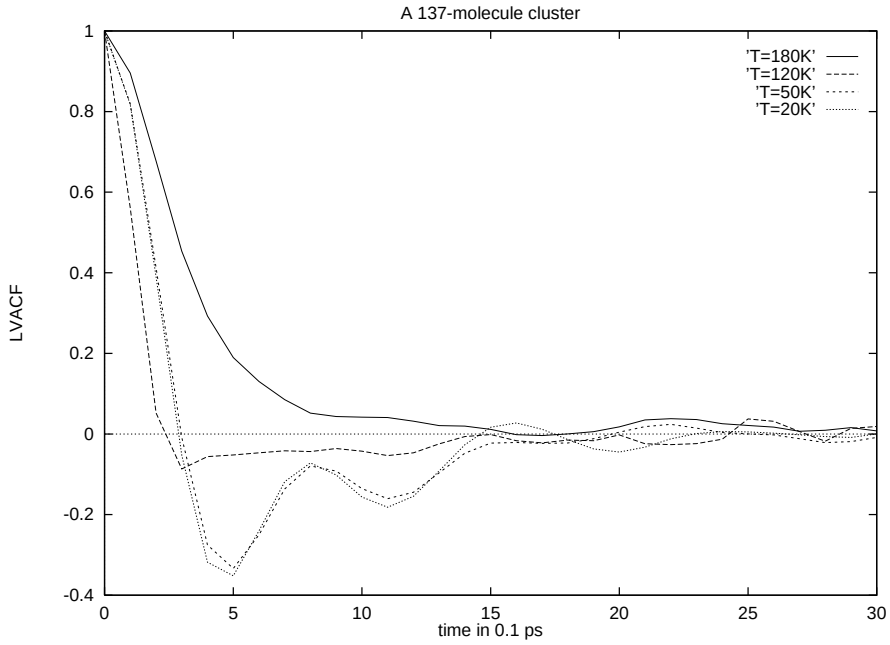

Fig. 2. The LVACF for a 137-molecule TeF_6 cluster at four selected temperatures: $T = 180\,\mathrm{K}$ (solid line), which is below the melting point, $T = 120\,\mathrm{K}$ (broken line), $T = 50\,\mathrm{K}$ (dashed line) below the first transition, which is at $T = 90\,\mathrm{K}$, $T = 20\,\mathrm{K}$ (dotted line) below the second transition, which takes place at about $T = 40\,\mathrm{K}$.

NMR method or Raman spectroscopy unless the temperature is moderately high. A Rayleigh scattering experiment would provide information about the collective reorientational motion (slow mode), which should be seen as a sharp peak superimposed on a broad background, because of rapid fluctuations of the molecules just above the transition temperature.

We have computed various correlation functions in order to elucidate the roles of the surface and volume contributions in the ordering process, which dictates the solid–solid transformations of plastic substances. Simulations were performed with $N = 30$, 51, 57, 81, 89, 128, 137, and 181 molecules in the temperature interval of 200–20 K. The temperature is changed in steps of 10 K away from the transition thermal region and in steps of 5 K (3 K for the smallest size) in the vicinity of the transition. Each run, at a specific average temperature achieved by velocity rescaling [15], is preceded by an equilibration of 10 ps, if the cluster is away from the transition, and of 50 ps, in the vicinity of the transition. The positions, velocities, orientations, angular velocities, forces, and torques for each molecule were stored at intervals of 10 time steps, i.e., 0.1 ps. We have prepared several starting configurations for each cluster size in order to average over the computed quantities. These configurations were obtained by the heating of the cluster at elevated temperatures, but below evaporation, which was encountered in some cases.

The normalized autocorrelation function for the variable A

$$C_A(t) = \langle A(0) \cdot A(t) \rangle / \langle A(0)^2 \rangle \,, \tag{2}$$

is calculated by subsequent analysis of the stored data. The rapidly relaxing ACF (velocity, angular velocity, force, torque) are calculated from all the data. The slowly relaxing orientational ACF are computed from the data taken every 10 or 20 time sequences of 10 time steps. The statistical precision of the computed correlation function can be slightly increased by averaging over $\tau_{\max}$ time origins:

$$C_A(t) = [1/\tau_{\max}] \sum_{t_0=1}^{\tau_{\max}} A(t_0) A(t_0 + t) \,. \tag{3}$$

3 Vibrational motion

The center-of-mass velocity ACF, $C_v(t)$, called hereafter the linear velocity autocorrelation function (LVACF), is given by

$$C_v(t) = \frac{m}{(3k_{\mathrm{B}}T)} \sum_{i=1}^{N} \langle v_i(t) \cdot v_i(0) \rangle \,, \tag{4}$$

where $v_i(t)$ is the velocity of the molecule at time t and m is the mass of a TeF_6 molecule, $m = 241.6$ a.u.m. The LVACF (4) is used to compute the diffusion coefficient D in the three-dimensional space:

$$D = \frac{1}{3N} \sum_{i=1}^{N} \int_0^{\infty} \mathrm{d}t \langle v_i(t) \cdot v_i(0) \rangle \,. \tag{5}$$

$C_v(t)$ is shown in Fig. 1 for clusters of two sizes at different temperatures. As the temperature is decreased, the negative portion of the curve appears to be due to rebound of a molecule against its neighbors.

Figure 1 shows the LVACF of an 89-molecule cluster at three different temperatures. At $\langle T \rangle = 120\,\mathrm{K}$, a temperature below the freezing limit (≈ 160–$170\,\mathrm{K}$) for this cluster size, the cluster is orientationally disordered with a short-range translational order somewhat broken at

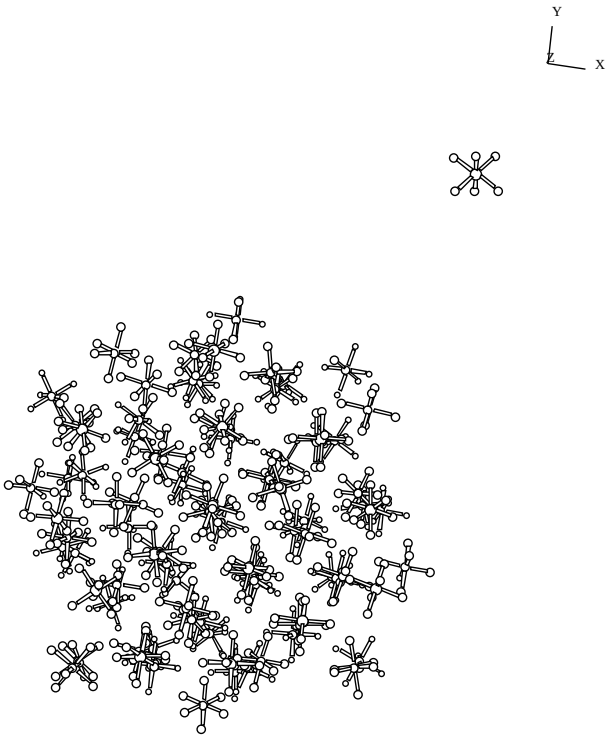

Fig. 3. A 89-molecule cluster at $T = 120$ K. The octahedral molecules have a short-range order and a complete orientational disorder. Tellurium atoms are in the center of the octahedron, and the fluorine atoms occupy the vertices.

the surface (Fig. 2). A small negative part is readily seen in Fig. 1 for $\langle T \rangle = 120$ K. The first transition is at $T_{\mathrm{trans1}} \simeq 80$ K for this size. In this transition, the bcc structure with orientational disorder transforms into a monoclinic structure with partial order. At $\langle T \rangle = 50$ K, the LVACF has a double minimum in its negative part. A partial order means that only one of the axes of symmetry of an octahedron is aligned [3]. This double minimum is an indication of the system's memory in the rebound of a molecule against its closest neighbors. At $\langle T \rangle = 20$ K, below the second transformation at $T_{\mathrm{trans2}} \simeq 40$ K, the two minima are well resolved, and the oscillating tail indicates the harmonic motion characteristic of a crystal.

The temperature dependence of the LVACF of a 137-molecule cluster is plotted in Fig. 3. As the linear size of the clusters of 89 and 137 molecules does not change too much (≈ 0.15), there is no significant change in the LVACF behavior either.

The temporal Fourier transform (FT) of the LVACF is proportional to the density of normal modes $\varrho(w)$ in a purely harmonic system, and is referred to as the "density of states" in solids. We have used a fast FT (FFT) algorithm [16] to compute the Fourier image of the autocorrelation functions. By increasing the length of the interval, over which we compute the ACF, we decrease the lower Nyquist frequency. The higher Nyquist frequency is defined by the time step of the records used in the computation of the correlation function. The lower limit of significance in the frequency spectrum is set by the duration of mechanical reversibility of the dynamics simulation, typically 5000–10 000 time steps.

The power spectrum of the LVACF of a 137-molecule cluster is shown in Fig. 6 for two temperatures: $\langle T \rangle = 100$ K is above the T_{trans1} temperature, and $\langle T \rangle = 70$ K is below it. Although the cluster is solid in the temperature interval (100–70 K), there are no sharp and well-resolved peaks in the frequency domain. The cause is the rotation–translation coupling that smears and shifts the peaks. Fur-

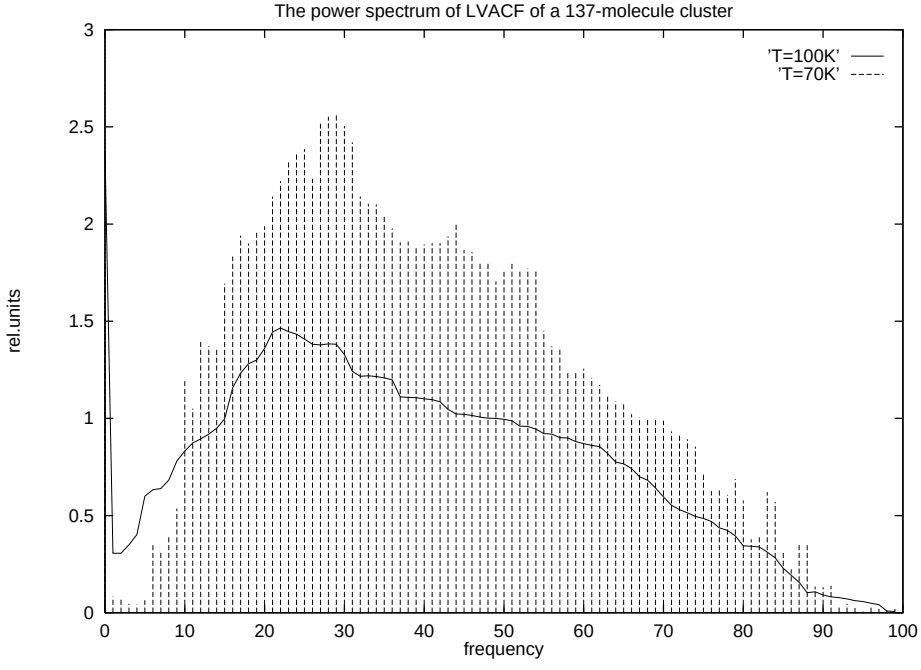

Fig. 4. The temperature dependence of the density of states (the Fourier images of the LVACF) for a 137-molecule cluster: (a) $T = 120$ K (dashed line), $T = 20$ K (dotted line); (b) $T = 120$ K (dashed line), $T = 70$ K (dotted line).

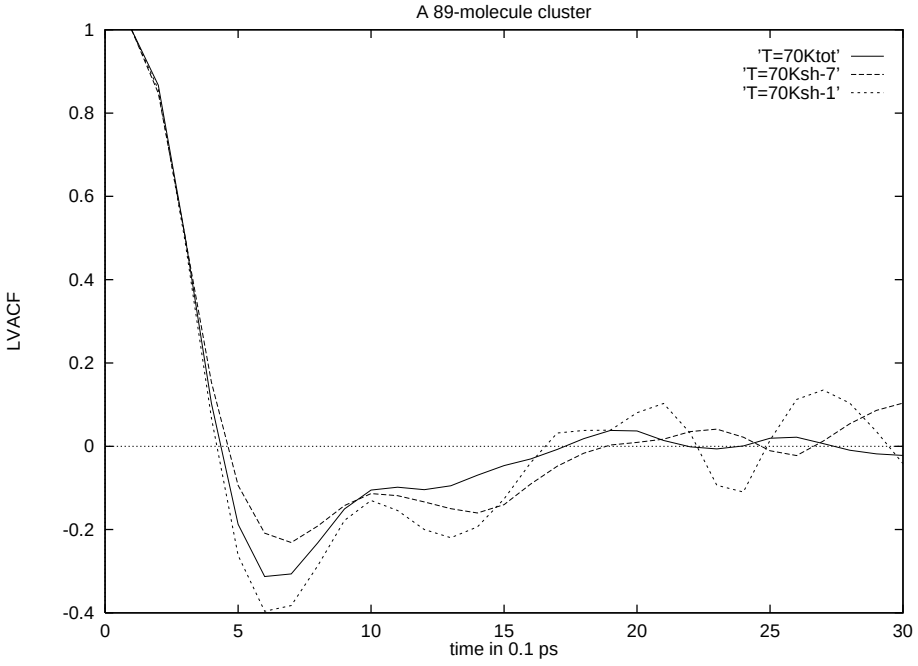

Fig. 5. The LVACF of a 89-molecule cluster at $T = 70$ K: The solid line is for all the molecules in the cluster; the broken line is for the first shell that contains 15 molecules having all their neighbors; and the dashed line is for the surface shell, consisting of 24 molecules. The surface dominates the behavior of the cluster as a whole.

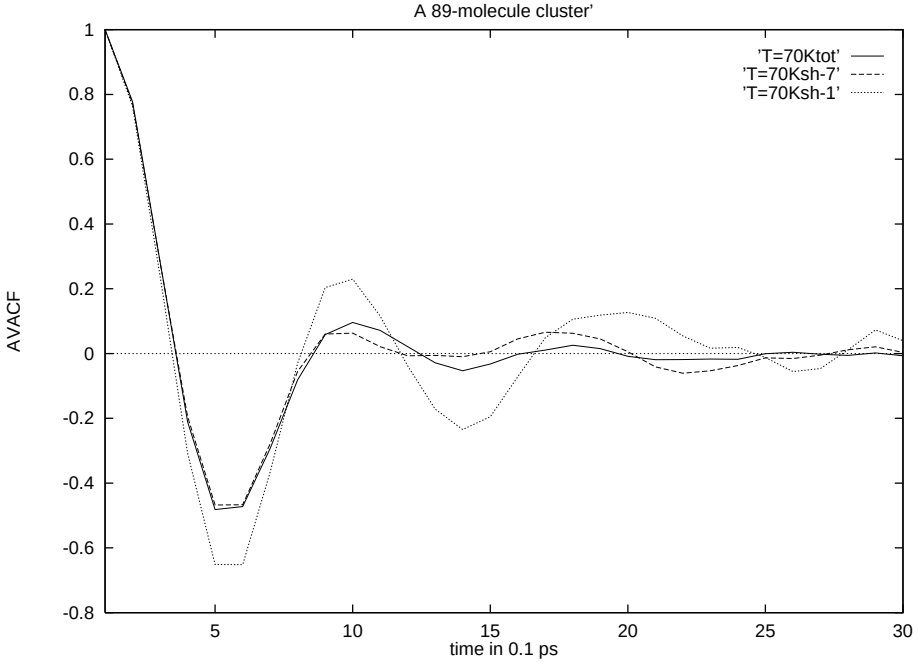

Fig. 6. The AVACF of a 89-molecule cluster at $T = 70$ K. The same notations are valid as for the case of LVACF.

ther study is needed to extract the exact value of the coupling constant.

4 The angular velocity ACF

The angular velocity ACF, $C_\omega(t)$, is defined as

$$C_\omega(t) = \sum_{i=1}^{N} \frac{\langle \omega_i(t) \cdot \omega_i(0) \rangle}{\langle \omega_i(0)^2 \rangle} \,, \qquad (6)$$

where ω_i is the angular velocity of molecule i in the space coordinate system. Since changes in angular velocity are induced by torques acting on a molecule, it is also useful to compute the torque autocorrelation function. The zero time value of the torque autocorrelation function can, in principle, be measured from the second and the fourth moments of the Raman line shape. The angular velocity ACF at $\langle T \rangle = 70$ K are shown in Fig. 6 for an 89-molecule cluster. The harmonic motion of the molecules is easily recognized. The negative portion of $C_\omega(t)$ is a necessary condition for the molecules to librate. However, the term "libration" can be reserved for cases where the integral over

the angular velocity correlation $D_\omega(t)$ is actually negative for some t:

$$D_\omega(t) = \int_0^t C_\omega(\tau)\mathrm{d}\tau. \quad (7)$$

The first positive portion C_ω dominates in the integral for most of the temperatures. Below the second transition, the integral becomes negative for very low temperatures. Two decay constants can be inferred from the angular velocity correlation function: for the surface molecules, $\tau_\mathrm{s} \approx 1.5$ ps, and for the volume molecules, $\tau_\mathrm{v} \approx 2.1$ ps.

Different experiments are sensitive to different properties of the rotational correlation functions. In a Raman measurement, the width of a low-frequency Lorentzian component in the line shape is related to the decay constant τ_dec obtained from (7). In the measurement, one deals with many clusters having different masses. The current analysis shows that the surface dominates the cluster behavior unless the temperature is not very low. As a result, the experiment will give only the decay constant corresponding to the surface molecules for temperatures above 20 K.

5 Conclusions

The analysis of the velocity autocorrelation functions indicates two characteristic decay times (memories) of finite systems: one related to the surface, and another related to the volume. Both the linear velocity and angular velocity autocorrelation functions have two negative minima at low temperatures for the volume molecules, while the surface molecules behave differently. Keeping in mind that the surface dominates the complete behavior of a small cluster at temperatures above 20 K, one should measure at very low temperatures in order to get information about the two constants. Otherwise, the surface decay constant will be measured. The distribution of the density of states (the power spectrum of the LVACF) does not show the shape typical for the bulk crystal solids. The reason for this is that the coupling of the rotational and translational degree of freedom is very important due to the symmetry breaking in free-surface finite systems.

We thank the Department of Energy for partial support during the completion of this work and the Department of Energy Institute for Nuclear Theory at the University of Washington for its hospitality. A.P. is grateful to Dr.C. Kohl for his help and valuable discussions.

References

1. A. Proykova, R.S. Berry: Z. Phys. D **40**, 215 (1997)
2. A. Proykova, R. Radev, Feng-Yin Li, R.S. Berry: J. Chem. Phys.**110**(8), 3887 (1999)
3. R.A. Radev, A. Proykova, Feng-Yin Li, R.S. Berry: J. Chem. Phys. **109**(9), 3596 (1998)
4. D. Frenkel, B. Mulder: Mol. Phys. **55**, 1171 (1985)
5. C.G. Windsor, D.H. Saunderson, J.N. Sherwood, D. Taylor, G.S. Pawley: J. Phys. C **11**, 1741 (1978)
6. G. Dolling, B.M. Powell, V.F. Sears: Mol. Phys. **37**, 1859 (1979)
7. L.S. Bartell, L. Harsami, E.J. Valente: NATO ASI Ser. B **158**, 37 (1987)
8. M.T. Dove, B.M. Powell, G.S. Pawley, L.S. Bartell: Mol. Phys. **65**, 353 (1988)
9. F.M. Beniere, A.H. Fuchs, M.F. de Feraudy, G. Torchet: Mol. Phys. **76**, 1071 (1992)
10. F.M. Beniere, A. Boutain, J.M. Simon, A.H. Fuchs, M.F. de Feraudy, G. Torchet: J. Phys. Chem. **97**, 10 472 (1993)
11. L.S. Bartell, F.J. Dulls, B. Chunko: J. Phys. Chem. **95**, 6481 (1991)
12. H. Reiss, P. Mirabel, R.L. Whetten: J. Phys. Chem. **92**, 7241 (1988)
13. A. Boutain, B. Rousseau, A.H. Fuchs: Chem. Phys. Lett. **218**, 122 (1994)
14. Feng-Yin Li, R.S. Berry, A. Proykova: in *Book of Abstracts of MWTCC*, May 12–16, Evanston, USA, ed. by M. Ratmer (1995), p. 33
15. J. Farges, M.F. de Feraudy, B. Raoult, G.J. Torchet: J. Chem. Phys. **78**, 5067 (1983)
16. J. Farges, M.F. de Feraudy, B. Raoult, G.J. Torchet: J. Chem. Phys. **84**, 3491 (1986)
17. R.M. Lynden-Bell, K.H. Michel: Rev. Mod. Phys. **66**, 721 (1994)
18. S. Nosé: Progr. Theor. Phys. Suppl. **103**, 1 (1991)
19. W. Press, B. Flannery, S. Teukolsky, W. Vetterling: *Numerical Recipes: The Art of Scientific Computing* (Cambridge University Press 1989)